The Plant Cell, Vol. 32: 4002–4016, December 2020, www.plantcell.org © 2020 ASPB.

Diverse Roles of the Salicylic Acid Receptors NPR1 and NPR3/NPR4 in Plant Immunity

Yanan Liu,[a,b,1] Tongjun Sun,[b,c,1] Yulin Sun,[b] Yanjun Zhang,[d] Ana Radojičić,[b] Yuli Ding,[b] Hainan Tian,[b] Xingchuan Huang,[a,b] Jiameng Lan,[b] Siyu Chen,[e] Alberto Ruiz Orduna,[f] Kewei Zhang,[d] Reinhard Jetter,[b,f] Xin Li,[b,c] and Yuelin Zhang[b,2]

[a] Hunan Provincial Key Laboratory of Phytohormones and Growth Development, College of Bioscience and Biotechnology, Hunan Agricultural University, Changsha 410128, China
[b] Department of Botany, University of British Columbia, Vancouver, British Columbia V6T 1Z4, Canada
[c] Michael Smith Laboratories, University of British Columbia, Vancouver, British Columbia V6T 1Z4, Canada
[d] Institute of Plant Genetics and Developmental Biology, College of Chemistry and Life Sciences, Zhejiang Normal University, Jinhua, Zhejiang 321004, China
[e] Key Laboratory of Molecular Epigenetics of Ministry of Education, Northeast Normal University, Changchun 130000, China
[f] Department of Chemistry, University of British Columbia, Vancouver, British Columbia V6T 1Z1, Canada

ORCID IDs: 0000-0001-9895-853X (Y.L.); 0000-0002-0263-3448 (T.S.); 0000-0002-9574-7179 (Y.S.); 0000-0002-7475-103X (Y.J.Z.); 0000-0003-0721-2033 (A.R.); 0000-0002-7299-5356 (Y.D.); 0000-0002-7497-5324 (H.T.); 0000-0001-8320-5615 (X.H.); 0000-0002-2187-3199 (J.L.); 0000-0001-8093-7167 (S.C.); 0000-0002-9066-0496 (A.R.O.); 0000-0002-0844-1121 (K.Z.); 0000-0002-6302-2835 (R.J.); 0000-0002-6354-2021 (X.L.); 0000-0002-3480-5478 (Y.Z.)

The plant defense hormone salicylic acid (SA) is perceived by two classes of receptors, NPR1 and NPR3/NPR4. They function in two parallel pathways to regulate SA-induced defense gene expression. To better understand the roles of the SA receptors in plant defense, we systematically analyzed their contributions to different aspects of Arabidopsis (*Arabidopsis thaliana*) plant immunity using the SA-insensitive *npr1-1 npr4-4D* double mutant. We found that perception of SA by NPR1 and NPR4 is required for activation of *N*-hydroxypipecolic acid biosynthesis, which is essential for inducing systemic acquired resistance. In addition, both pattern-triggered immunity (PTI) and effector-triggered immunity (ETI) are severely compromised in the *npr1-1 npr4-4D* double mutant. Interestingly, the PTI and ETI attenuation in *npr1-1 npr4-4D* is more dramatic compared with the *SA-induction deficient2-1* (*sid2-1*) mutant, suggesting that the perception of residual levels of SA in *sid2-1* also contributes to immunity. Furthermore, NPR1 and NPR4 are involved in positive feedback amplification of SA biosynthesis and regulation of SA homeostasis through modifications including 5-hydroxylation and glycosylation. Thus, the SA receptors NPR1 and NPR4 play broad roles in plant immunity.

INTRODUCTION

Plants have evolved diverse mechanisms to defend themselves against microbial pathogen infections. Plants perceive pathogens by pattern-recognition receptors or resistance (R) proteins at the infection sites, which triggers the activation of local defenses that lead to a secondary immune response in distal tissues termed systemic acquired resistance (SAR; Jones and Dangl, 2006; Fu and Dong, 2013; Zhou and Zhang, 2020). Pattern-recognition receptors recognize conserved molecules present in groups of microorganisms during pattern-triggered immunity (PTI), collectively known as microbe-associated molecular patterns (Zipfel, 2014). For example, the conserved 22-amino acid flg22 peptide, derived from the N terminus of bacterial flagellin, is recognized by the receptor kinase FLAGELLIN-SENSITIVE2 (Gómez-Gómez and Boller, 2000). At the same time, plant R proteins detect fast-evolving effector proteins secreted from pathogens and used for colonization, leading to the activation of effector-triggered immunity (ETI; Cui et al., 2015; Li et al., 2015). Most *R* genes encode nucleotide binding leucine-rich repeat receptors (NLRs; Li et al., 2015). Typical NLRs can be classified into two subgroups based on their N-terminal domains: Toll/Interleukin1 Receptor-type NLRs (TNLs) and Coiled Coil-type NLRs (CNLs). Differential signaling events occur downstream of TNLs and CNLs. ENHANCED DISEASE SUSCEPTIBILITY1 (EDS1) is essential for immunity mediated by TNLs, while NON-RACE-SPECIFIC DISEASE RESISTANCE1 (NDR1) is required for disease resistance activated by some CNLs (Aarts et al., 1998).

Salicylic acid (SA) is a phytohormone with critical roles in both local defense and SAR (Vlot et al., 2009; Zhang and Li, 2019). In Arabidopsis (*Arabidopsis thaliana*), SA is perceived by two classes of receptors: NONEXPRESSER OF PR GENES1 (NPR1) and NPR1-LIKE PROTEIN 3 (NPR3)/NPR4, which activate two parallel signaling pathways to stimulate the expression of defense-related genes and immunity (Fu et al., 2012; Wu et al., 2012; Ding et al., 2018). As NPR family proteins do not contain DNA binding domains, NPR1 and NPR3/NPR4 must interact with the transcription factors TGACG SEQUENCE-SPECIFIC

[1] These authors contributed equally to this work.
[2] Address correspondence to yuelin.zhang@ubc.ca.
The author responsible for distribution of materials integral to the findings presented in this article in accordance with the policy described in the Instructions for Authors (www.plantcell.com) is: Yuelin Zhang (yuelin.zhang@ubc.ca).
www.plantcell.org/cgi/doi/10.1105/tpc.20.00499

IN A NUTSHELL

Background: Plants use a set of proteins that localize to the cell-surface, called Pattern Recognition Receptors (PRRs), as well as intracellular Resistance (R) proteins, to sense and respond to pathogen attacks. PRRs recognize critical pathogen components and activate Pattern-triggered immunity (PTI). Successful pathogens can themselves deliver effector proteins into plant cells to inhibit PTI. As a counteracting measure, R proteins can also detect effectors directly or indirectly, initiating effector-triggered immunity (ETI). In addition, pathogen infections at the local site can activate systemic acquired resistance (SAR), which mounts a long-lasting and effective defense against a wide range of pathogens throughout the entire plant. The defense phytohormone Salicylic acid (SA) is critical in this process and is perceived by two groups of receptors, NPR1 and NPR3/NPR4 in *Arabidopsis thaliana*. Furthermore, N-hydroxypipecolic acid (NHP) serves as a mobile signal in the context of SAR.

Question: How does SA perception contribute to PTI, ETI and SAR?

Findings: We used the SA-insensitive *npr1-1 npr4-4D* double mutant, which is thought to completely block SA perception in Arabidopsis. We discovered that perception of SA by the two groups of dedicated receptors contributes to the induction of NHP biosynthetic genes and, thus, production of NHP during pathogen infection. In addition, SA perception by NPR1 and NPR4 contributes additively to PTI and ETI. Finally, SA perception also plays critical roles in regulating the biosynthesis and catabolism of SA.

Next steps: SA induces NHP production through SA receptors, but how NHP promotes SA biosynthesis and SA-induced resistance in tissues distal from the infection site is unclear. The future identification of NHP receptor(s) will be crucial in the dissection of this part of the pathway.

BINDING PROTEIN (TGA) TGA2/TGA5/TGA6 for signal transduction (Zhang et al., 1999; Després et al., 2000; Zhou et al., 2000; Zhang et al., 2006). NPR1 functions as a transcriptional activator (Fan and Dong, 2002; Rochon et al., 2006), and binding of SA to NPR1 promotes its activity (Wu et al., 2012; Ding et al., 2018). NPR3/NPR4, by contrast, serve as transcriptional repressors to repress the expression SA-responsive genes in the absence of pathogen infection. Binding of SA to NPR3/NPR4 inhibits their transcriptional repressor activity, leading to derepression of their target genes and activation of defense (Ding et al., 2018). In addition to transcriptional repression, NPR3/NPR4 were also proposed to function in the regulation of NPR1 stability (Fu et al., 2012).

In land plants, SA is synthesized from shikimate through either Phe or isochorismate (Huang et al., 2020). Upon pathogen infection, SA levels in Arabidopsis plants drastically increase due to enhanced SA biosynthesis through the isochorismate pathway (Wildermuth et al., 2001; Rekhter et al., 2019). The expression of *SA-DEFICIENT2* (*SID2*), which encodes the SA biosynthesis enzyme ISOCHORISMATE SYNTHASE1 (ICS1), is rapidly induced (Wildermuth et al., 2001). The induction of *SID2/ICS1* by pathogens is largely facilitated by the transcription factors SYSTEMIC ACQUIRED RESISTANCE DEFICIENT1 (SARD1) and CAM BINDING PROTEIN60-LIKE g (CBP60g; Wang et al., 2009, 2011; Zhang et al., 2010). Loss of SARD1 or CBP60g results in dramatic reduction of *ICS1* induction and SA biosynthesis. In addition to *ICS1*, two other SA biosynthesis genes, *avrPphB SUSCEPTIBLE3* (*PBS3*) and *EDS5*, are also transcriptionally regulated by SARD1 and CBP60g (Sun et al., 2015).

2,5-Dihydroxybenzoic acid (2,5-DHBA) is a major SA catabolite, and its formation through SA hydroxylation plays a critical role in maintaining SA homeostasis (Zhang et al., 2017). *DOWNY MILDEW RESISTANT6* (*DMR6*) encodes an SA 5-hydroxylase (S5H) that converts SA to 2,5-DHBA (Zhang et al., 2017). In *dmr6* mutant plants, SA cannot be converted to 2,5-DHBA, leading to elevated SA levels and enhanced disease resistance (van Damme et al., 2008; Zhang et al., 2017). During senescence, Arabidopsis plants also accumulate high levels of 2,3-DHBA (Zhang et al., 2017), due to the conversion of SA catalyzed by an SA 3-hydroxylase (S3H) that is paralogous to DMR6/S5H (Zhang et al., 2013). In the *s5h s3h* double mutant, SA levels further increase compared with the *dmr6* single mutant, leading to severe dwarfism and autoimmunity (Zhang et al., 2017). Despite the importance of *DMR6* in maintaining SA levels, it is currently unknown how it is transcriptionally regulated.

In addition to SA, *N*-hydroxypipecolic acid (NHP) and its precursor pipecolic acid (Pip) also play key roles in plant immune signaling and are required for SAR (Navarova et al., 2012; Chen et al., 2018; Hartmann et al., 2018). Pip is biosynthesized from Lys in two sequential reactions catalyzed by the amino acid transferase AGD2-LIKE DEFENSE RESPONSE PROTEIN1 (ALD1) and the reductase SARD4 (Ding et al., 2016; Hartmann et al., 2017). FLAVIN-DEPENDENT MONOOXYGENASE1 (FMO1) further converts Pip into NHP, which most likely serves as a mobile signal for SAR (Chen et al., 2018; Hartmann et al., 2018). Upon pathogen infection, *ALD1*, *SARD4*, and *FMO1* expression is dramatically induced, leading to increased biosynthesis of Pip and NHP. The induction of *ALD1*, *SARD4*, and *FMO1*, and thus of Pip and NHP biosynthesis, also depends on SARD1 and CBP60g (Sun et al., 2015, 2018, 2020). Furthermore, the transcription factor WRKY33 is similarly involved in the induction of *ALD1* and Pip biosynthesis during infection by *Pseudomonas syringae* pv *tomato* (*Pto*) DC3000 *avrRpt2* (Wang et al., 2018).

Here, we systematically examined the roles of SA and its receptors in PTI, ETI, and SAR by taking advantage of the *npr1-1 npr4-4D* double mutant, which blocks both SA perception pathways. We determined that both activation of NPR1 and inhibition of NPR3/NPR4 by SA are required for SAR and contribute to PTI and ETI. In addition, SA perception also plays critical roles in regulating the biosynthesis and catabolism of NHP and SA.

RESULTS

Regulation of SAR and NHP Levels by the SA Receptors NPR1 and NPR4

Arabidopsis NPR1 was previously shown to be required for SAR (Cao et al., 1994). To test whether SAR is affected in the gain-of-function SA-insensitive mutant *npr4-4D*, we compared SAR responses in wild-type Columbia-0 (Col-0), *npr1-1*, *npr4-4D*, and *npr1-1 npr4-4D* plants using a previously developed SAR assay (Zhang et al., 2010). As shown in Figure 1, the bacterial pathogen

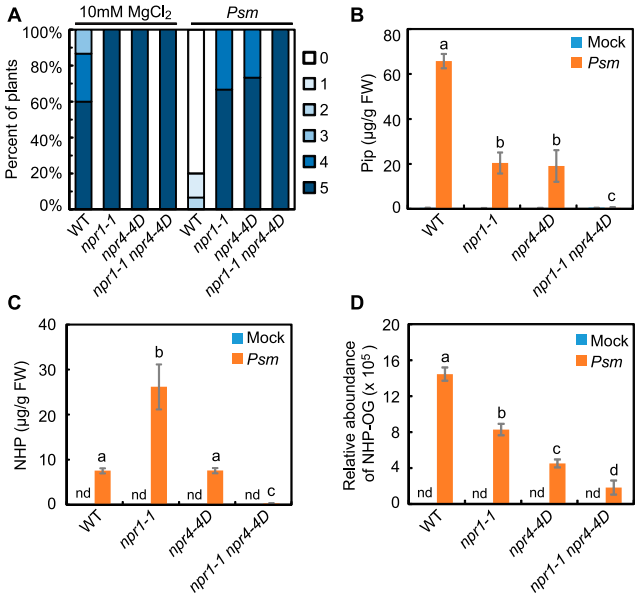

Figure 1. Regulation of SAR and NHP Levels by NPR1 and NPR4.

(A) Growth of *Hpa* Noco2 on the distal leaves of wild-type Col-0, *npr1-1*, *npr4-4D*, and *npr1-1 npr4-4D* plants in a SAR assay. Two primary leaves of 3-week-old plants were infiltrated with *Psm* ES4326 (OD_{600} = 0.001) or 10 mM $MgCl_2$ (mock) 2 d before the plants were sprayed with *Hpa* Noco2 spore suspension (50,000/mL in water). We included 15 plants for each treatment. Disease symptoms were scored 7 d later by counting the number of conidiophores on the distal leaves. Disease ratings are as follows: 0, no conidiophores on plants; 1, one leaf is infected with no more than five conidiophores; 2, one leaf is infected with more than five conidiophores; 3, two leaves are infected but with no more than five conidiophores on each infected leaf; 4, two leaves are infected with more than five conidiophores on each infected leaf; 5, more than two leaves are infected with more than five conidiophores. The experiment was repeated three times with independently grown plants, yielding similar results.
(B) and **(C)** Amounts of Pip **(B)** and NHP **(C)** in leaf tissue for the indicated genotypes 24 h after infiltration with *Psm* ES4326 (OD_{600} = 0.001) or 10 mM $MgCl_2$ (Mock).
(D) Amounts of NHP-*O*G in leaf samples 24 h after treatment with *Psm* ES4326 (OD_{600} = 0.001) or 10 mM $MgCl_2$ (Mock).
For **(B)** to **(D)**, error bars represent SD of three independent biological replicates from 4-week-old plants. Different letters indicate samples with statistical differences ($P < 0.05$, Student's *t* test; $n = 3$). FW, fresh weight; nd, not detectable. These experiments were repeated twice with independently grown plants, yielding similar results.

Pseudomonas syringae pv *maculicola* (*Psm*) ES4326 induced SAR in wild-type plants, as it conferred strong resistance against the virulent oomycete pathogen *Hyaloperonospora arabidopsidis* (*Hpa*) Noco2, whereas *npr1-1* plants showed severely compromised SAR, consistent with a previous report (Zhang et al., 2010). Notably, SAR was also severely compromised in *npr4-4D* and completely lost in the *npr1 npr4-4D* double mutant, suggesting that constitutive repression of SA signaling in *npr4-4D* dampens SAR, and both branches of SA signaling are required for SAR.

Although SA is known to be required for SAR, how it affects SAR is unclear. Since NHP serves as the likely mobile signal for SAR, we tested whether SA signaling contributes to the biosynthesis of NHP and its precursor Pip. We measured Pip and NHP levels in the wild type and the *npr* mutants after infection by *Psm* ES4326. Pip levels were much lower in *npr1-1* and *npr4-4D* plants than in the wild type and were reduced to trace amounts in the *npr1-1 npr4-4D* double mutant (Figure 1B), suggesting that NPR1 and NPR4 regulate Pip accumulation in response to pathogen infection. In agreement with a previous report, NHP levels significantly increased in *npr1-1* compared with the wild type (Hartmann et al., 2018), whereas *npr4-4D* plants accumulated similar amounts of NHP as the wild type. However, the *npr1-1 npr4-4D* double mutant accumulated very little NHP after *Psm* ES4326 infection (Figure 1C), indicating that NPR1 and NPR4 function in parallel to regulate pathogen-induced NHP accumulation. Further analysis showed that *O*-glycosylated NHP (NHP-OG) levels significantly decreased in *npr1-1* and *npr4-4D* plants relative to the wild type and dropped further in *npr1-1 npr4-4D* (Figure 1D).

Regulation of the Expression of NHP Biosynthetic Genes by NPR1 and NPR4

As we observed lower NHP levels in *npr1-1 npr4-4D* plants, we next tested whether NPR1 and NPR4 regulate the expression of the NHP biosynthesis genes *ALD1*, *SARD4*, and *FMO1* upon infection by examining their transcript levels in *npr1-1*, *npr4-4D*, and *npr1 npr4-4D* plants infiltrated with *Psm* ES4326. Consistent with Pip levels, the *Psm* ES4326-mediated induction of *ALD1* and *SARD4* expression was greatly reduced in *npr4-4D* and almost completely abolished in *npr1-1 npr4-4D* plants (Figures 2A and 2B). By contrast, induction of *FMO1* by *Psm* ES4326 was comparable in *npr1-1* and wild-type plants but greatly reduced in *npr4-4D* and was further decreased in *npr1-1 npr4-4D* (Figure 2C). These findings suggest that NPR1 and NPR4 independently regulate the expression of NHP biosynthesis genes. As the transcript levels of *ALD1*, *SARD4*, and *FMO1* are not higher in *npr1-1* than in the wild type, the increased NHP accumulation in *npr1-1* shown in Figure 1C is unlikely to be due to increased NHP biosynthesis.

To examine whether SA induces the expression of NHP biosynthetic genes, we first checked a transcriptome deep sequencing (RNA-seq) data set for SA-induced gene expression in the wild type and *npr* mutants (Ding et al., 2018). *ALD1*, *SARD4*, and *FMO1* were among the genes significantly induced by SA in wild-type plants. To validate the RNA-seq data, we measured the expression of these three genes before and after SA treatment by

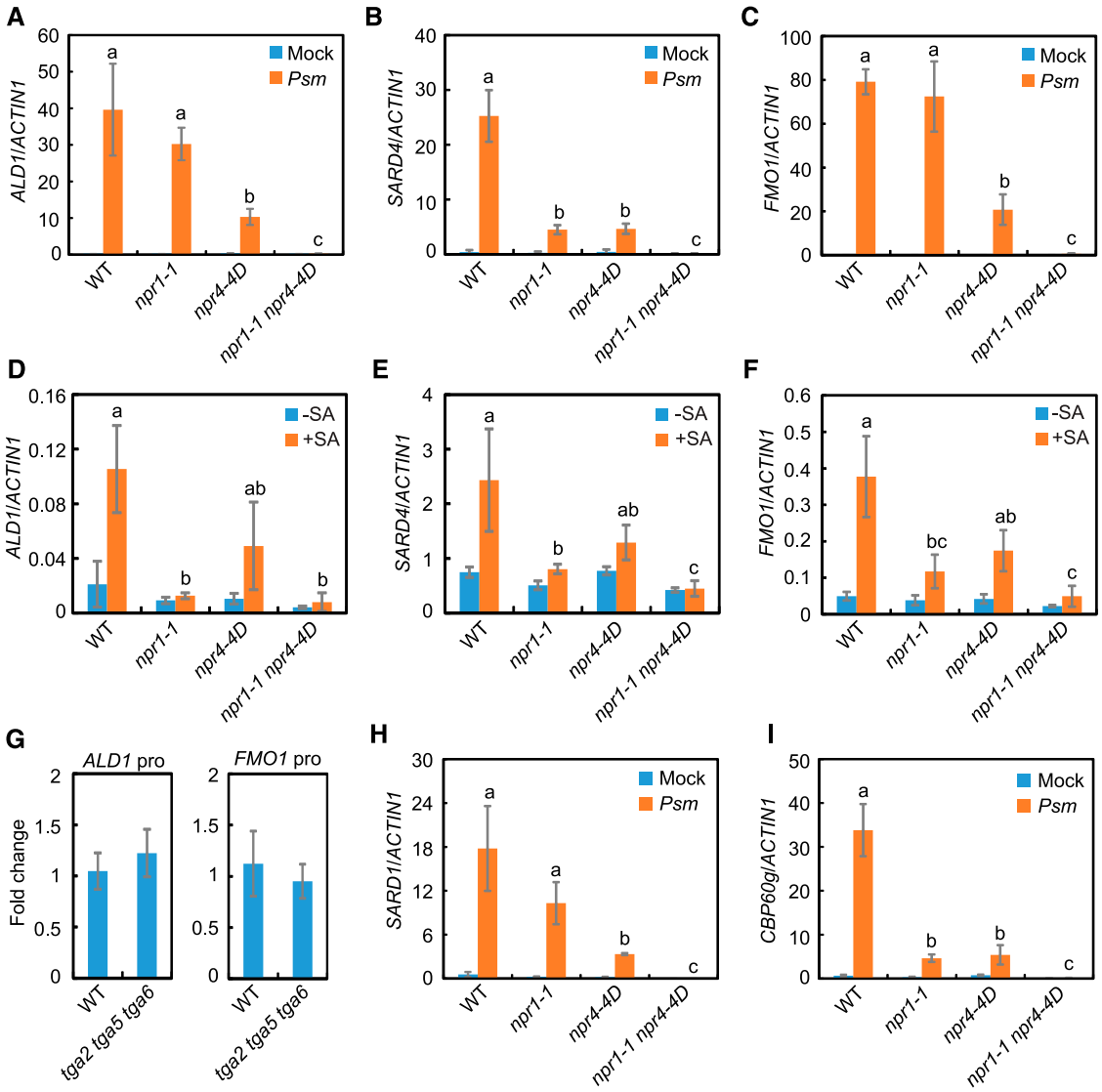

Figure 2. Regulation of *ALD1*, *SARD4*, and *FMO1* Transcript Levels by NPR1 and NPR4.

(A) to **(C)** Induction of *ALD1* **(A)**, *SARD4* **(B)**, and *FMO1* **(C)** expression in the leaves of 4-week-old wild-type Col-0, *npr1-1*, *npr4-4D*, and *npr1-1 npr4-4D* plants 24 h after infiltration with *Psm* ES4326 (OD_{600} = 0.001) or 10 mM $MgCl_2$ (Mock).

(D) to **(F)** Induction of *ALD1* **(D)**, *SARD4* **(E)**, and *FMO1* **(F)** expression in 2-week-old seedlings for wild-type Col-0, *npr1-1*, *npr4-4D*, and *npr1-1 npr4-4D* before (0 h) and after (1 h) treatment with 50 μM SA.

(G) Binding of TGA2 to the *ALD1* and *FMO1* promoter regions, as determined by ChIP experiments. ChIP was performed using anti-TGA2 antibodies and protein A-agarose beads or protein A-agarose beads alone (no-antibody control). For each genotype, we calculated the fold change of ChIP signal for anti-TGA2 antibodies relative to the no-antibody control. Data represent measurements of four samples from two independent experiments. No statistical differences were detected between ChIP signals from the wild type and *tga2 tga5 tga6* for each promoter tested (Student's *t* test; $n = 4$).

(H) and **(I)** Induction of *SARD1* **(H)** and *CBP60g* **(I)** expression in leaf tissue of 4-week-old wild-type Col-0, *npr1-1*, *npr4-4D*, and *npr1-1 npr4-4D* plants 24 h after infiltration with *Psm* ES4326 (OD_{600} = 0.001) or 10 mM $MgCl_2$ (Mock).

Values were normalized to *ACTIN1* expression. Error bars represent SD of three independent biological replicates. Different letters indicate samples with statistical differences: $P < 0.01$ (**[A]** to **[C]**) and $P < 0.05$ (**[D]** to **[F]**, **[H]**, and **[I]**), Student's *t* test ($n = 3$).

RT-qPCR. As shown in Figures 2D to 2F, SA strongly induced the expression of these three genes, and the induction was significantly lower in *npr1-1* and further reduced in the *npr1-1 npr4-4D* double mutant. Thus, SA and SA perception are required for pathogen-induced NHP biosynthesis.

As NPR proteins interact with TGA transcription factors for signaling, we next examined whether TGAs might contribute to the induction of NHP biosynthetic genes. Sequence analysis identified a single TGACG motif in the promoter regions of *ALD1* and *FMO1* but none in the *SARD4* promoter (Supplemental Table 1).

We performed chromatin immunoprecipitation (ChIP)-qPCR analysis using anti-TGA2 antibodies to determine whether TGA transcription factors are targeted to the *ALD1* and *FMO1* promoters. As shown in Figure 2G, we detected no significant enrichment of *ALD1* or *FMO1* promoter DNA fragments in the immunoprecipitated chromatin samples. Together, these data suggest that *ALD1* and *FMO1*, as well as *SARD4*, are most likely not direct targets of TGA2/TGA5/TGA6.

SARD1 and CBP60g are known to directly regulate the expression of *ALD1*, *SARD4*, and *FMO1* (Wang et al., 2009; Zhang et al., 2010; Sun et al., 2015, 2018), prompting us to check whether their induction by *Psm* ES4326 is dependent on SA signaling. As shown in Figures 2H and 2I, the *npr1-1 npr4-4D* double mutant almost completely blocked the induction of both *SARD1* and *CBP60g*, indicating that NPR1 and NPR4 likely modulate the expression of *ALD1*, *SARD4*, and *FMO1* through SARD1 and CBP60g.

Perception of SA by NPR1 and NPR4 Is Required for NHP-Induced Immunity

Because NHP induces the expression of SA biosynthetic genes (Chen et al., 2018; Hartmann et al., 2018), we examined whether the perception of SA by NPR1 and NPR4 may be required for NHP-induced immunity. We first infiltrated primary leaves with 1 mM NHP and later spray-inoculated the entire plants with a spore suspension of *Hpa* Noco2. As shown in Figure 3A, we observed very little growth of the pathogen on wild-type plants pretreated with NHP, suggesting that NHP induces strong resistance against *Hpa* Noco2. By contrast, NHP-pretreated *npr1-1*, *npr4-4D*, *npr1-1 npr4-4D*, and *sid2-1* plants remained susceptible to *Hpa* Noco2, indicating that SA signaling is required for NHP-induced immunity.

To confirm that SA perception is required for NHP-triggered immunity, we crossed the *npr1-1* and *npr4-4D* mutants with the

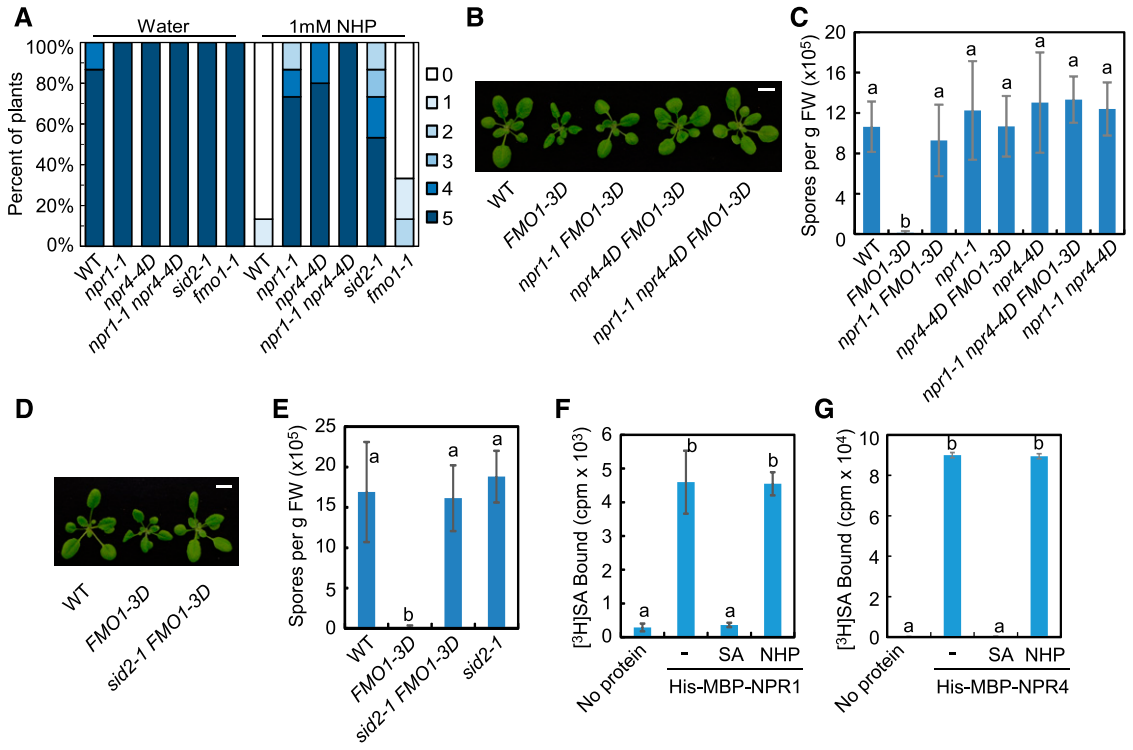

Figure 3. Roles of NPR1 and NPR4 in NHP-Induced Immunity.

(A) NHP-induced immunity against *Hpa* Noco2 in wild-type Col-0, *npr1-1*, *npr4-4D*, *npr1-1 npr4-4D*, *sid2-1*, and *fmo1-1* plants. Two primary leaves from 3-week-old plants were infiltrated with 1 mM NHP or water 1 d before plants were sprayed with *Hpa* Noco2 spore suspension (50,000/mL in water). A total of 15 plants were scored for each treatment. Disease symptoms were scored 7 d later using the disease rating scores (0 to 5) described in Figure 1A.
(B) Morphology of 3-week-old wild-type Col-0, *FMO1-3D*, *npr1-1 FMO1-3D*, *npr4-4D FMO1-3D*, and *npr1-1 npr4-4D FMO1-3D* plants. Bar = 1 cm.
(C) Growth of *Hpa* Noco2 in 2-week-old seedlings of the indicated genotypes.
(D) Morphology of 3-week-old wild-type Col-0, *FMO1-3D*, and *sid2-1 FMO1-3D* plants. Bar = 1 cm.
(E) Growth of *Hpa* Noco2 on 2-week-old wild-type Col-0, *FMO1-3D*, *sid2-1 FMO1-3D*, and *sid2-1* seedlings.
Error bars in **(C)** and **(E)** represent SD of four independent biological replicates. Different letters indicate samples with statistical differences ($P < 0.01$, Student's *t* test; $n = 4$). FW, fresh weight. For **(A)**, **(C)**, and **(E)**, the experiments were repeated twice using independently grown plants, with similar results.
(F) and **(G)** Effects of excessive amounts of unlabeled SA or NHP on binding of recombinant NPR1 **(F)** and NPR4 **(G)** proteins to [^{3}H]SA in size-exclusion chromatography. A total of 0.4 mg/mL purified His6-MBP-NPR1 or His6-MBP-NPR4 protein was incubated with 200 nM [^{3}H]SA in 50 μL of PBS buffer with or without a 10,000-fold excess amount of unlabeled SA or NHP. A sample with no protein added (No protein) was used as a negative control. Error bars represent SD of three independent reactions. Different letters indicate samples with statistical differences ($P < 0.01$, Student's *t* test; $n = 3$). Experiments were repeated twice using different batches of recombinant proteins, with similar results.

FMO1-3D mutant, where *FMO1* is overexpressed and defense responses are constitutively activated, presumably due to increased NHP biosynthesis (Koch et al., 2006). As shown in Figure 3B, *FMO1-3D* exhibited morphological phenotypes such as stunted growth and curly leaves typically associated with autoimmunity. These phenotypes were partially suppressed in the *npr1-1 FMO1-3D* and *npr4-4D FMO1-3D* double mutants and completely suppressed in the *npr1-1 npr4-4D FMO1-3D* triple mutant. In addition, the *npr1-1* and *npr4-4D* mutations also blocked the enhanced resistance against *Hpa* Noco2 normally seen in the *FMO1-3D* background (Figure 3C). Similarly, the dwarfism and enhanced immunity of *FMO1-3D* plants were also suppressed by the *sid2-1* mutation (Figures 3D and 3E). Together, these data further underscore that SA signaling is required for NHP-activated immunity.

Since the NHP and SA molecules have similar structures, with six-membered rings carrying carboxyl and hydroxyl substituents in a 1,2-constellation, we tested whether NHP might bind to NPR proteins like SA. We performed [^{3}H]SA-NPR binding assays in the presence of excessive amounts of unlabeled substrates. As shown in Figures 3F and 3G, the addition of unlabeled SA outcompeted the binding of [^{3}H]SA to NPR1 and NPR4 proteins, while the addition of unlabeled NHP had no effect, suggesting that NHP probably does not bind directly to NPR1/NPR4, at least not through the same binding sites as SA.

Perception of SA by Both NPR1 and NPR4 Is Required for PTI

Since *npr* mutants were shown to support enhanced growth of the nonpathogenic bacterium *Pto* DC3000 *hrcC* (Ding et al., 2018), we analyzed the contributions of the two branches of SA signaling to PTI, using the *sid2-1* mutant as a control. As shown in Figure 4A, flg22-induced protection against *Pto* DC3000 was compromised in *npr1-1* and *npr4-4D* to a similar extent and was further reduced in *npr1-1 npr4-4D*, suggesting that perception of SA by NPR1 and NPR4 contributes to flg22-induced immunity. Surprisingly, flg22-induced protection against *Pto* DC3000 was more drastically reduced in *npr1-1 npr4-4D* than in *sid2-1*, suggesting that PTI is more severely compromised in *npr1-1 npr4-4D* than in *sid2-1*. Such phenotypic differences between SA biosynthesis and SA perception mutants indicate a major function of the residual SA in *sid2-1* for PTI.

In wild-type plants, the expression of *SARD1*, *PATHOGENESIS-RELATED1* (*PR1*), and *PR2* is strongly induced by treatment with *Pto* DC3000 *hrcC*. Here, we documented a significant reduction of this induction in *npr1-1* and *npr4-4D* and an almost complete loss in *npr1-1 npr4-4D* (Figures 4B to 4D), suggesting that the perception of SA by NPR1 and NPR4 is required for the expression of defense genes during PTI. Although *sid2-1* blocked *Pto* DC3000 *hrcC*-induced *PR1* expression, we still detected some induction of *SARD1* and *PR2* in *sid2-1*, suggesting that the residual SA contributes to defense gene expression during PTI.

Perception of SA by NPR1 and NPR4 Is Required for ETI

Next, we examined the contribution of the two SA signaling pathways in ETI by comparing the growth of the avirulent bacterial strains *Pto* DC3000 *AvrRpt2* and *Pto* DC3000 *AvrRps4* in wild-type, *npr1-1*, *npr4-4D*, *npr1-1 npr4-4D*, and *sid2-1* plants. These two bacterial strains trigger immunity mediated by the CNL RPS2 and the TNL RPS4, respectively. As shown in Figure 4E, the growth of both pathogens significantly increased in *npr1-1* and *npr4-4D* relative to the wild type and increased even further in *npr1-1 npr4-4D*, suggesting that perception of SA by NPR1 and NPR4 is important for ETI. The *npr1-1 npr4-4D* double mutant supported a 34-fold higher growth of *Pto* DC3000 *AvrRpt2* and a 12-fold higher growth of *Pto* DC3000 *AvrRps4* than the *sid2-1* mutant, indicating that defense conferred by the residual SA in *sid2-1* is also critical for ETI.

Treatment with *Pto* DC3000 *AvrRpt2* or *Pto* DC3000 *AvrRps4* in the wild type dramatically induced the expression of the defense-related genes *SARD1*, *PR1*, and *PR2* (Figures 4F to 4H). Induction of all three genes was drastically reduced in *npr1-1 npr4-4D*. By contrast, the induction of *SARD1* and *PR2* remained largely unaffected in *sid2-1* and only the expression of *PR1* was *SID2*-dependent, suggesting that the residual SA in *sid2-1* contributes to defense gene expression during ETI.

PTI and ETI Are More Severely Compromised in *npr1-1 npr4-4D* Than in *fmo1-1 sid2-1* Mutants

Since mutations in *npr1-1* and *npr4-4D* not only directly affect SA perception but also indirectly influence NHP production during pathogen infection (Figure 1C), we tested whether the severe PTI and ETI defects in *npr1-1 npr4-4D* are due to synergistic effects between SA signaling defects and reduced NHP levels. To this end, we compared *npr1-1 npr4-4D* with the *fmo1-1 sid2-1* double mutant, in which NHP- and pathogen-induced SA biosynthesis are blocked. As shown in Figure 5, growth of *Pto* DC3000 *hrcC* did not change in *fmo1-1*, *sid2-1*, and *fmo1-1 sid2-1* but reached considerably higher levels in *npr1-1 npr4-4D*. flg22-induced protection against *Pto* DC3000 was reduced in both *npr1-1 npr4-4D* and *fmo1-1 sid2-1* but was much more pronounced in *npr1-1 npr4-4D* (Figure 5B). Consistent with a previous report in which mutations in *fmo1-1* and *sid2-1* had additive effects on ETI (Bartsch et al., 2006), growth of *Pto* DC3000 *AvrRpt2* and *Pto* DC3000 *AvrRps4* was significantly higher in the *fmo1-1 sid2-1* double mutant than in the single mutants (Figures 5C and 5D). However, growth of the two avirulent bacterial strains was even higher in *npr1-1 npr4-4D* than in *fmo1-1 sid2-1*. These results further underscore the important roles played by residual SA in *sid2-1* during PTI and ETI.

NPR1 and NPR4 Regulate SA Hydroxylation by Controlling *DMR6* Expression

Arabidopsis *npr1* mutant plants have been shown to accumulate higher levels of SA than the wild type (Delaney et al., 1995); however, it was unclear whether this increase is only due to enhanced biosynthesis or also due to reduced catabolism. To test whether NPR1 and NPR4 are involved in the regulation of SA catabolism, we quantified 2,5-DHBA levels in wild-type, *npr1-1*, *npr4-4D*, and *npr1-1 npr4-4D* plants. As shown in Figure 6, basal 2,5-DHBA levels were significantly lower in *npr1-1* and *npr4-4D*

and greatly reduced in *npr1-1 npr4-4D* plants compared with the wild type. Similarly, 2,5-DHBA levels after pathogen infection also decreased in *npr1-1* and *npr4-4D* single mutants and reached much lower levels in the *npr1-1 npr4-4D* double mutant. These results suggest that both NPR1 and NPR4 are involved in regulating the production of 2,5-DHBA, which is a major SA catabolite.

Next, we examined whether the expression of *DMR6*, which encodes a 5-hydroxylase converting free SA into 2,5-DHBA

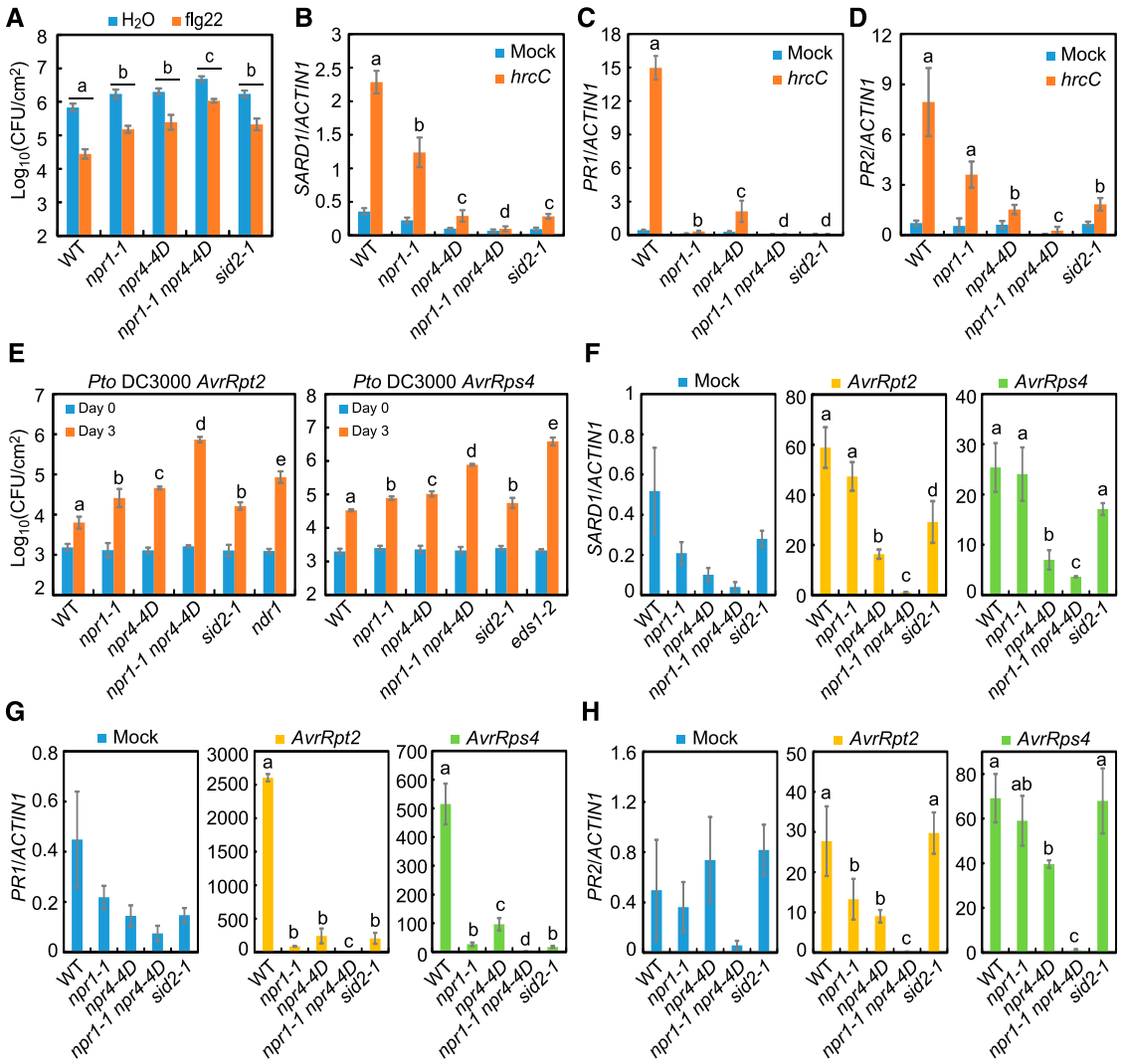

Figure 4. Regulation of PTI and ETI by NPR1 and NPR4.

(A) Growth of *Pto* DC3000 on the leaves of 4-week-old wild-type Col-0, *npr1-1*, *npr4-4D*, *npr1-1 npr4-4D*, and *sid2-1* plants after treatment with water or 1 μM flg22. After 24 h, the treated leaves were infiltrated with *Pto* DC3000 (OD_{600} = 0.001). Samples were taken 3 d after *Pto* DC3000 inoculation. Error bars represent SD from six biological replicates. The reduction of bacterial titer after flg22 treatment in each genotype was regarded as flg22-induced protection. The flg22-induced protection among different genotypes was compared using a two-way ANOVA test, and different letters indicate genotypes with statistical differences ($P < 0.05$, Student's *t* test; $n = 6$). The experiment was repeated twice with independently grown plants, with similar results. CFU, colony-forming units.

(B) to **(D)** Induction of *SARD1* **(B)**, *PR1* **(C)**, and *PR2* **(D)** expression in the indicated genotypes 12 h after infiltration with *Pto* DC3000 *hrcC* or 10 mM $MgCl_2$ (Mock).

(E) Growth of *Pto* DC3000 *AvrRpt2* and *Pto* DC3000 *AvrRps4* in the indicated genotypes. Error bars represent SD from six biological replicates. Different letters indicate samples with statistical differences ($P < 0.05$, Student's *t* test; $n = 6$). The experiment was repeated three times with independently grown plants, with similar results.

(F) to **(H)** Induction of *SARD1* **(F)**, *PR1* **(G)**, and *PR2* **(H)** expression in the indicated genotypes 16 h after infiltration with 10 mM $MgCl_2$ (Mock), *Pto* DC3000 *AvrRpt2*, and *Pto* DC3000 *AvrRps4*.

In **(B)** to **(D)** and **(F)** to **(H)**, values were normalized to *ACTIN1*. Error bars represent SD from three independent biological replicates. Different letters indicate samples with statistical differences ($P < 0.05$, Student's *t* test; $n = 3$). Plants used in all assays were 4 weeks old.

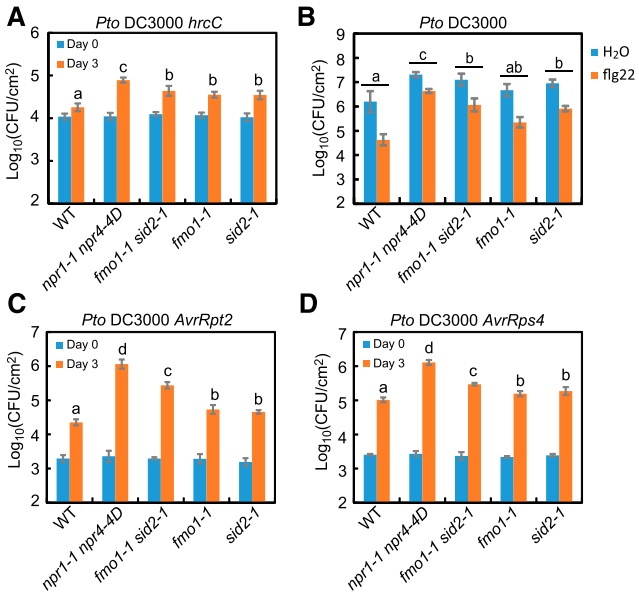

Figure 5. Analysis of Immune Defects in *npr1-1 npr4-4D* and *fmo1-1 sid2-1* Double Mutants.

(A) Growth of *Pto* DC3000 *hrcC* in wild-type Col-0, *npr1-1 npr4-4D*, *fmo1-1 sid2-1*, *fmo1-1*, and *sid2-1* plants.

(B) Growth of *Pto* DC3000 in the indicated genotypes after treatment with water or flg22. The experiment was performed as described in Figure 4A. The flg22-induced protection (the reduction of bacterial titer after flg22 treatment in each genotype) among different genotypes was compared using a two-way ANOVA test.

(C) and **(D)** Growth of *Pto* DC3000 *AvrRpt2* **(C)** and *Pto* DC3000 *AvrRps4* **(D)** for the indicated genotypes.

Error bars represent SD from six biological replicates. Different letters indicate samples with statistical differences ($P < 0.05$, Student's *t* test; $n = 6$). Experiments were repeated twice with independently grown plants, with similar results. Plants used in all assays were 4 weeks old. CFU, colony-forming units.

(Zhang et al., 2017), is regulated by NPR1 and NPR4. Analysis of a previously generated RNA-seq data set (Ding et al., 2018) showed that the expression of *DMR6* was induced by SA in wild-type plants, which we confirmed by RT-qPCR analysis (Figure 6B). The induction of *DMR6* by SA was completely blocked in *npr1-1 npr4-4D* (Figure 6B). We also measured the expression levels of *DMR6* in wild-type and *npr* mutant plants treated with *Pto* DC3000 *AvrRpt2*. In the mock treatment, the expression of *DMR6* was significantly lower in *npr1-1* and *npr4-4D* than in the wild type and was further reduced in *npr1-1 npr4-4D* (Figure 6C). Following infection by *Pto* DC3000 *AvrRpt2*, *DMR6* expression was strongly induced in the wild type, and this induction was reduced in *npr1-1* as well as *npr4-4D* and completely blocked in the *npr1-1 npr4-4D* double mutant. Together, these data suggest that NPR1 and NPR4 regulate SA catabolism by modulating *DMR6* expression.

Since both NPR1 and NPR4 work with the redundant TGA transcription factors TGA2, TGA5, and TGA6 to regulate SA-induced gene expression (Zhang et al., 1999, 2003, 2006; Després et al., 2000), we examined the expression of *DMR6* in the *tga2 tga5 tga6* triple mutant with or without SA treatment. Consistent with the requirement of TGA2/TGA5/TGA6 for the transcriptional repression of SA-responsive genes by NPR3/NPR4 (Ding et al., 2018), the basal expression level of *DMR6* was much higher in the *tga2 tga5 tga6* triple mutant than in the wild type (Figure 6D). However, treatment with SA did not further induce *DMR6* in *tga2 tga5 tga6* plants, suggesting that TGAs may be involved in the induction of *DMR6* by SA.

In the promoter region of *DMR6*, we identified two TGACG motifs that are 9 bp apart (Supplemental Table 1). To determine whether *DMR6* is a direct target of TGAs, we performed ChIP-qPCR experiments on wild-type and *tga2 tga5 tga6* plants using anti-TGA2 antibodies. qPCR analysis of the immunoprecipitated DNA revealed that *DMR6* promoter fragments were significantly enriched by anti-TGA2 antibodies in wild-type plants but not in *tga2 tga5 tga6* plants (Figure 6E), suggesting that the transcription factors TGA2/TGA5/TGA6 directly bind to the *DMR6* promoter region and thus, together with the SA receptors, regulate the expression of *DMR6*.

NPR1 and NPR4 Regulate the Production of SAG and SA

As SA can also be glycosylated into SA 2-O-β-D-glucoside (SAG), we examined whether NPR1 and NPR4 regulate the production of SA as well as SAG. We measured and compared the levels of free SA and SAG in the wild type, *npr1-1*, *npr4-4D*, and *npr1 npr4-4D*. As shown in Figure 6F, under mock treatment, SAG levels were significantly higher in *npr1-1*, *npr4-4D*, and *npr1 npr4-4D* than in the wild type, suggesting that decreased SA 5-hydroxylation in *npr1-1* and *npr4-4D* mutant plants may be compensated by increased SA glycosylation. The levels of free SA after infection by *Pto* DC3000 *AvrRpt2* were comparable in the wild type, *npr4-4D*, and *npr1 npr4-4D* but were considerably higher in *npr1-1*, consistent with a previous report (Delaney et al., 1995). SAG levels after *Pto* DC3000 *AvrRpt2* infection were similar in the wild type and *npr1-1* but were significantly lower in *npr4-4D* and were further reduced in the *npr1-1 npr4-4D* double mutant. These results suggest that NPR1 and NPR4 regulate SA accumulation as well as the conversion of SA to SAG.

There are at least three UDP-glucosyltransferases (UGTs) involved in the conversion of SA to SAG in Arabidopsis. Of those, UGT74F1 and UGT76B1 have high glucosyltransferase activity, whereas UGT74F2 shows very low glucosyltransferase activity (Noutoshi et al., 2012). Therefore, we focused our analysis on *UGT74F1* and *UGT76B1*. As shown in Supplemental Figure 1, the expression of *UGT74F1* was not induced upon infection by *Pto* DC3000 *AvrRpt2*, consistent with previous findings that *UGT74F1* is expressed at low but constitutive levels and is barely induced by biotic stresses (Noutoshi et al., 2012). In comparison, the expression of *UGT76B1* was dramatically induced by *Pto* DC3000 *AvrRpt2* in wild-type plants, but the induction was greatly reduced in *npr1-1* and *npr4-4D* and was almost completely blocked in *npr1-1 npr4-4D* (Figure 6G). While SA also induced *UGT76B1* expression in the wild type, this induction was greatly reduced in *npr1-1* and *npr4-4D* and was completely blocked in *npr1-1 npr4-4D* (Figure 6H), suggesting that NPR1 and NPR4 are involved in regulating the expression of *UGT76B1*.

We further analyzed the expression levels of *UGT76B1* l in the *tga2 tga5 tga6* triple mutant before and after SA treatment. As

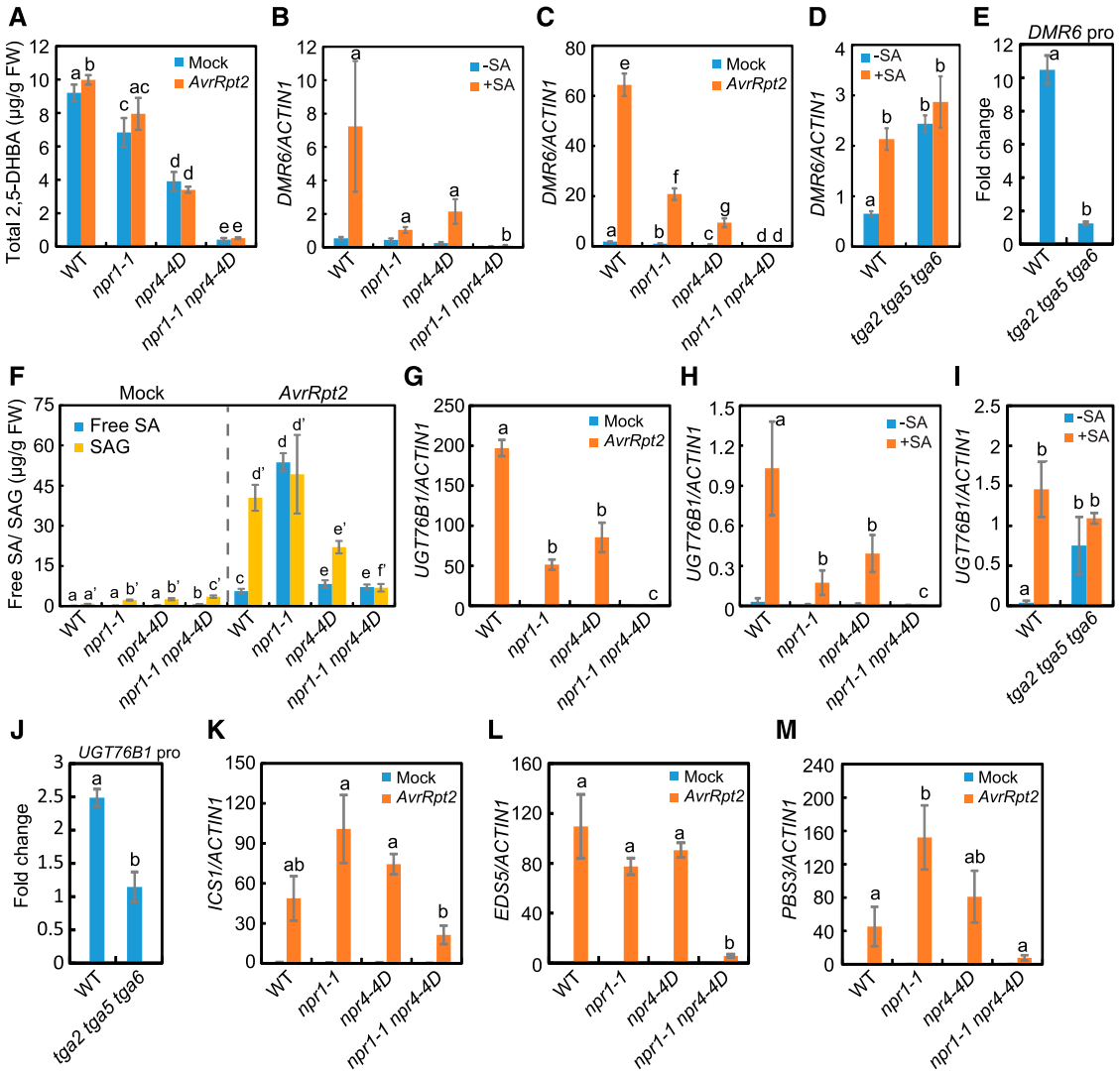

Figure 6. Regulation of SA Biosynthesis, Hydroxylation of SA, and Conversion of SA to SAG by NPR1 and NPR4.

(A) Levels of 2,5-DHBA in 4-week-old wild-type Col-0, *npr1-1*, *npr4-4D*, and *npr1-1 npr4-4D* plants treated with 10 mM $MgCl_2$ (Mock) or *Pto* DC3000 *AvrRpt2*.

(B) SA-induced expression of *DMR6* in 2-week-old seedlings of the indicated genotypes.

(C) Induction of *DMR6* expression in the leaves of 4-week-old plants of the indicated genotypes 16 h after infiltration with 10 mM $MgCl_2$ (Mock) or *Pto* DC3000 *AvrRpt2*.

(D) SA-induced expression of *DMR6* in 2-week-old wild-type Col-0 and *tga2 tga5 tga6* seedlings.

(E) Binding of TGA2 to the *DMR6* promoter region, as determined by ChIP-qPCR.

(F) Levels of free SA and SAG in 4-week-old plants of the indicated genotypes treated with 10 mM $MgCl_2$ (Mock) or *Pto* DC3000 *AvrRpt2*.

(G) Induction of *UGT76B1* expression in the leaves of 4-week-old plants of the indicated genotypes 16 h after infiltration with 10 mM $MgCl_2$ (Mock) or *Pto* DC3000 *AvrRpt2*.

(H) SA-induced expression of *UGT76B1* in 2-week-old seedlings of the indicated genotypes.

(I) SA-induced expression of *UGT76B1* in 2-week-old wild-type Col-0 and *tga2 tga5 tga6* seedlings.

(J) Binding of TGA2 to the *UGT76B1* promoter region, as determined by ChIP-qPCR.

(K) to **(M)** Induction of *ICS1* **(K)**, *EDS5* **(L)**, and *PBS3* **(M)** expression in the leaves of 4-week-old plants of the indicated genotypes 16 h after infiltration with 10 mM $MgCl_2$ (Mock) or *Pto* DC3000 *AvrRpt2*.

For **(A)** and **(F)**, error bars represent SD from four independent biological replicates. Different letters indicate samples with statistical differences ($P < 0.05$, Student's *t* test; $n = 4$). FW, fresh weight. These experiments were repeated three times with similar results. For **(B)**, **(D)**, **(H)**, and **(I)**, 2-week-old seedlings were sprayed with 50 μM SA. RNA samples were collected before (−SA) and 1 h after (+SA) treatment. For **(B)** to **(D)**, **(G)** to **(I)**, and **(K)** to **(M)**, values were normalized to *ACTIN1*. Error bars represent SD from three independent biological replicates. Different letters indicate samples with statistical differences ($P < 0.05$, Student's *t* test; $n = 3$). For **(E)** and **(J)**, ChIP was performed using anti-TGA2 antibodies and protein A-agarose beads or protein A-agarose beads with

shown in Figure 6I, the expression level of *UGT76B1* in *tga2 tga5 tga6* was much higher than in the wild type but was not further induced by SA treatment. There are two TGACG motifs in the *UGT76B1* promoter region (Supplemental Table 1), and ChIP-qPCR analysis showed that DNA from this region was enriched by anti-TGA2 antibodies in samples from the wild type but not *tga2 tga5 tga6* (Figure 6J). These results suggest that TGA2, TGA5, and TGA6 directly regulate the expression of *UGT76B1* together with the SA receptors.

We also tested whether NPR1 and NPR4 regulate the expression of SA biosynthetic genes. As shown in Figures 6K and 6L, the expression of *ICS1*, *EDS5*, and *PBS3* was dramatically induced by *Pto* DC3000 *AvrRpt2* in the wild type, but this induction was significantly reduced in the *npr1-1 npr4-4D* double mutant. SA treatment also induced the expression of *ICS1*, *EDS5*, and *PBS3* in the wild type but not in *npr1-1 npr4-4D* (Supplemental Figures 2A to 2C), suggesting that SA positively regulates its own biosynthesis through its receptors NPR1 and NPR4. Notably, the expression levels of *ICS1* and *PBS3* were significantly higher in *npr1-1* than in the wild type after infection by *Pto* DC3000 *AvrRpt2*, indicating a negative role of NPR1 besides its positive feedback function on SA biosynthesis.

Even though TGACG motifs are present in the promoter regions of *ICS1*, *EDS5*, and *PBS3* (Supplemental Table 1), DNA from the TGACG motif-containing regions was not significantly enriched by anti-TGA2 antibodies in ChIP-qPCR experiments (Supplemental Figures 2D to 2F), suggesting that NPR1 and NPR4 regulate the expression of SA biosynthetic genes either indirectly or by interacting with other transcription factors that bind to their promoter regions. The induction of *ICS1*, *EDS5*, and *PBS3* was previously shown to be directly regulated by the transcription factors SARD1 and CBP60g. As shown in Figure 4F and Supplemental Figure 3, the expression of *SARD1* and *CBP60g* was significantly reduced in the *npr1-1 npr4-4D* double mutant upon infection by *Pto* DC3000 *AvrRpt2*, suggesting that NPR1 and NPR4 likely regulate pathogen-induced SA biosynthesis by modulating the expression of *SARD1* and *CBP60g*.

DISCUSSION

Since the early characterization of transgenic plants expressing the salicylate hydroxylase gene *NahG* from *Pseudomonas putida*, in which SA is converted to catechol (Gaffney et al., 1993; Delaney et al., 1994), it has long been established that SA is required for SAR. However, how SA contributes to SAR activation is still not fully understood. Here, analysis of the SA perception-deficient *npr1-1 npr4-4D* double mutant revealed that SA perception is essential for the induction of NHP biosynthetic genes and the production of NHP during pathogen infection. This is most likely through the SA-mediated upregulation of *SARD1* and *CBP60g*, which encode two transcription factors that directly control the expression of the NHP biosynthesis genes *ALD1*, *SARD4*, and *FMO1* (Sun et al., 2015, 2018). Since NHP functions as a mobile signal for SAR (Chen et al., 2018; Hartmann et al., 2018), one of the contributions of SA to SAR is to induce the production of the mobile signal in local tissue (Figure 7). As SAR induced by NHP treatment and resistance against *Hpa* Noco2 in *FMO1-3D* are blocked by mutations in *npr1-1* and *npr4-4D*, the perception of SA by NPR1 and NPR4 is also required for NHP-induced defense responses, in addition to promoting NHP biosynthesis (Figure 7). NHP was previously shown to induce the expression of *SARD1* and *CBP60g* as well as SA biosynthetic genes (Chen et al., 2018; Hartmann et al., 2018). Most likely, NHP activates SA-mediated immunity by promoting SA biosynthesis.

In *npr1-1* mutant plants infected with *Psm* ES4326, the expression of *FMO1* is unaffected but the NHP level is considerably higher than in the wild type (Figure 1C). The increased NHP accumulation in *npr1-1* may be due to reduced conversion of NHP to NHP-*O*G, as NHP-*O*G abundance in *npr1-1* is significantly lower than in the wild type (Figure 1D). In *npr4-4D* mutant plants infected with *Psm* ES4326, although the expression of *FMO1* is dramatically reduced, NHP levels are similar to those in wild-type plants, which may be explained by reduced conversion of NHP to NHP-*O*G in *npr4-4D* (Figure 1C). UGT76B1 was recently reported to function as an NHP glucosyltransferase (Bauer et al., 2020; Mohnike et al., 2020; Sattely et al., 2020). Since SA induces the expression of *UGT76B1* (Figure 6H), the reduced conversion of NHP to NHP-*O*G in the *npr1-1* and *npr4-4D* mutants is most likely due to reduced expression of *UGT76B1*.

As flg22-induced resistance against *Pto* DC3000 is compromised in the *npr1-1* and *npr4-4D* mutants and further reduced in the *npr1-1 npr4-4D* double mutant, both NPR1-dependent and NPR4-dependent SA signaling are important, and both contribute additively to PTI. This hypothesis is supported by the reduced induction of defense gene expression (Figures 4B to 4D) and the increased growth of *Pto* DC3000 *hrcC* in *npr1-1*, *npr4-4D*, and *npr1-1 npr4-4D* (Ding et al., 2018). Interestingly, the reduction of flg22-induced resistance against *Pto* DC3000 in *npr1-1 npr4-4D* is even more dramatic than in the SA-deficient mutant *sid2-1*. The *npr1-1 npr4-4D* double mutant also supports considerably higher growth of *Pto* DC3000 *hrcC* than *sid2-1*, and the induction of *SARD1* and *PR2* by *Pto* DC3000 *hrcC* is significantly lower in *npr1-1 npr4-4D* than in *sid2-1*. These data suggest that perception of the residual SA in *sid2-1* by the SA receptors contributes to a *SID2*-independent PTI response.

It was shown previously that *npr1-1 npr4-4D* exhibits enhanced cell death upon *Pto* DC3000 *AvrRpt2* infection, suggesting that SA signaling negatively regulates cell death during ETI (Radojičić et al., 2018). An analysis of the growth of *Pto* DC3000 *AvrRpt2* and *Pto* DC3000 *AvrRps4* showed that they are modestly increased in the *npr1-1* and *npr4-4D* single mutants but are much higher in the *npr1-1 npr4-4D* double mutant (Figure 4E), suggesting that both NPR1-dependent and NPR4-dependent SA signaling pathways contribute to resistance against avirulent pathogens. Notably,

Figure 6. (continued).

no antibody added (no-antibody control). For each genotype, fold change of the ChIP signal for anti-TGA2 antibodies was calculated relative to the no-antibody control. The results represent measurements of four samples from two independent experiments. Different letters indicate samples with statistical differences ($P < 0.01$, Student's t test; $n = 4$).

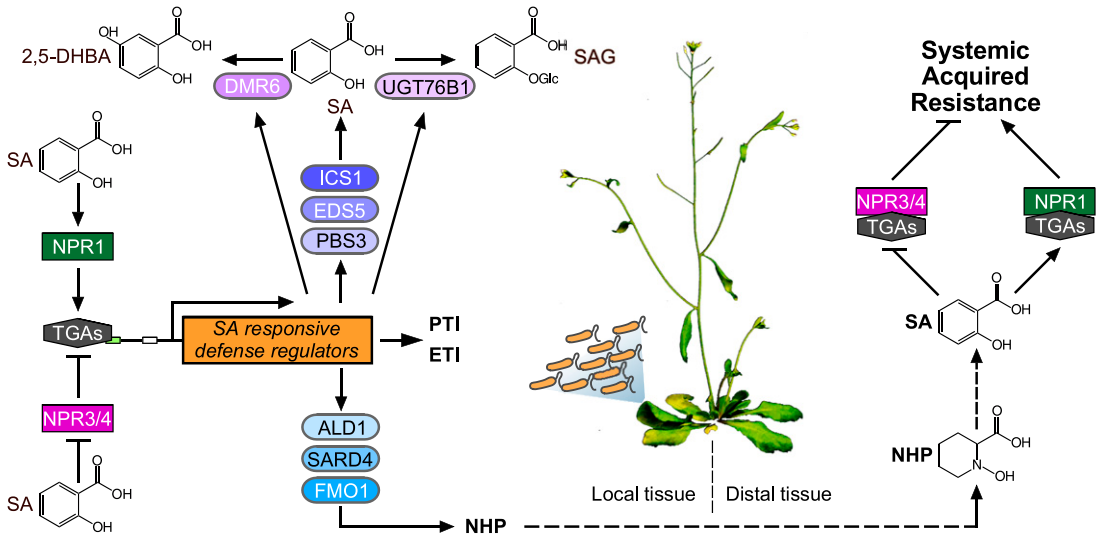

Figure 7. A Working Model Summarizing the Broad Roles of SA Receptors in Plant Immunity.

SA is perceived by two classes of receptors: NPR1 and NPR3/NPR4. Binding of SA abolishes the transcriptional repression activity of NPR3/NPR4 and enhances the transcriptional activation activity of NPR1, leading to the upregulation of SA-responsive defense regulators. The induction of SA biosynthetic genes (*ICS1*, *EDS5*, and *PBS3*) promotes SA production, whereas the induction of *UGT76B1* and *DMR6* stimulates the conversion of SA to 2,5-DHBA and SAG, respectively. In local tissues, the expression of SA-responsive defense regulators promotes both PTI and ETI and stimulates the production of the SAR mobile signal NHP by activating the expression of NHP biosynthetic genes (*ALD1*, *SARD4*, and *FMO1*). In distal tissues, NHP promotes SA biosynthesis and SA-induced resistance.

growth of the two bacterial strains is over 10-fold higher in *npr1-1 npr4-4D* than in *sid2-1*, suggesting that the perception of a basal level of SA in *sid2-1* by NPR1 and NPR4 is also critical for ETI. This observation is further supported by the much lower expression of defense-related genes in *npr1-1 npr4-4D* than in *sid2-1* during infection by the avirulent bacteria (Figures 4F to 4H).

Since *SID2* is required for pathogen-induced SA biosynthesis (Wildermuth et al., 2001), immune responses in *sid2* mutant plants have been considered as evidence of SA-independent defense in previous studies. However, our findings showed that blocking SA perception has a much more severe effect on both ETI and PTI than loss of SID2 function, suggesting that residual SA content in *sid2-1* plays critical roles in plant immunity. As SA perception promotes NHP production, and since the *fmo1-1 sid2-1* double mutant is more susceptible to *Pto* DC3000 *AvrRpt2* and *Pto* DC3000 *AvrRps4* than the *sid2-1* single mutant, the severely compromised ETI in *npr1-1 npr4-4D* may be partially due to reduced NHP accumulation. However, both ETI and PTI are more severely compromised in *npr1-1 npr4-4D* than in *fmo1-1 sid2-1*, suggesting that residual SA in *sid2-1* also contributes to plant defenses independently of NHP. Considering that defense-related genes controlled by NPR1 and NPR3/NPR4 are not up-regulated in the absence of pathogen, even though the in vitro binding constants of NPR1 and NPR3/NPR4 (ranging from ~20 to 200 nM) are considerably lower than the estimated basal levels of free SA (~1.4 μM; Ding et al., 2018), the activities of the SA receptors are most likely subject to posttranscriptional regulation in planta. It is possible that certain protein modifications induced at early stages of pathogen attack enable them to respond to basal levels of SA.

In addition to their roles in PTI, ETI, and SAR, we determined that NPR1 and NPR4 are also involved in regulating the conversion of SA to 2,5-DHBA and SAG, two major SA derivatives contributing to SA homeostasis. *DMR6* and *UGT76B1*, which encode an S5H and an SA glycosyltransferase, respectively (Noutoshi et al., 2012; Zhang et al., 2017), are target genes of the NPR1/NPR4-interacting transcription factors TGA2/TGA5/TGA6. Their expression is strongly induced by SA, suggesting that they are directly regulated by the SA receptors. Consistent with the expression levels of *DMR6*, 2,5-DHBA levels in *npr1-1* and *npr4-4D* are significantly lower than in the wild type and are further reduced in the *npr1-1 npr4-4D* double mutant. In *npr1-1 npr4-4D*, induction of *UGT76B1* and accumulation of SAG following infection by *Pto* DC3000 *AvrRpt2* are also dramatically reduced. These findings indicate that NPR1 and NPR4 play key roles in the negative feedback regulation of SA accumulation by controlling the production of 2,5-DHBA and SAG (Figure 7).

In the *npr1-1 npr4-4D* double mutant, the induction of SA biosynthetic genes and the accumulation of SA upon induction by *Pto* DC3000 *AvrRpt2* are significantly lower than in the wild type. The lower induction of SA biosynthetic genes in *npr1-1 npr4-4D* is most likely due to reduced expression of the genes encoding the transcription factors SARD1 and CBP60g (Figure 4F; Supplemental Figure 3), which directly regulate the expression of *ICS1*, *EDS5*, and *PBS3*, whose transcripts are also induced by SA. These findings suggest a positive feedback amplification loop in which the perception of SA stimulates its own biosynthesis (Figure 7). The involvement of SA receptors in both positive regulation of SA biosynthesis and negative regulation of SA accumulation through SA hydroxylation and glycosylation is likely important for spatial and temporal regulation of SA levels, which is an interesting area to explore in the future.

It was previously shown that SA levels in *npr1* mutant plants are significantly higher than in the wild type, indicating that NPR1 plays

a negative role in regulating SA levels (Delaney et al., 1995). However, the mechanism by which NPR1 affects SA levels was unclear. The reduced accumulation of 2,5-DHBA in *npr1-1* suggests that increased SA accumulation in *npr1* mutant plants is partly due to the reduced hydroxylation of SA by DMR6. SAG levels in *npr1-1* after *Pto* DC3000 *AvrRpt2* infection are comparable to the free SA levels, in contrast to wild-type plants, which accumulate much higher SAG than SA, suggesting that the mutant has also reduced conversion of SA to SAG, contributing to the increased free SA accumulation. Furthermore, increased SA biosynthesis most likely also contributes to higher SA levels in *npr1* mutants, as the expression levels of *ICS1* and *PBS3* following infection by *Pto* DC3000 *AvrRpt2* are significantly higher in *npr1-1* than in the wild type. How loss of function of NPR1 leads to increased *ICS1* and *PBS3* expression remains to be determined in the future.

In summary, the SA receptors NPR1 and NPR3/NPR4 play diverse roles in plant immunity by regulating SA-responsive defense-related genes (Figure 7). The perception of SA promotes both PTI and ETI and is required for activating NHP biosynthesis in local tissue and NHP-induced defense responses during SAR. In addition, the SA receptors are involved in positive feedback amplification of SA biosynthesis as well as SA 5-hydroxylation and glycosylation, enabling fine-tuned regulation of SA levels during plant immunity.

METHODS

Plant Materials and Growth Conditions

All plants used in this study are in the Arabidopsis (*Arabidopsis thaliana*) accession Col-0 background. The *npr1-1*, *npr4-4D*, *npr1-1 npr4-4D*, *tga2 tga5 tga6*, *fmo1-3D*, *fmo1-1*, *sid2-1*, *fmo1-1 sid2-1*, *ndr1-1*, and *eds1-2* mutants were described previously (Cao et al., 1994; Century et al., 1995; Wildermuth et al., 2001; Zhang et al., 2003; Bartsch et al., 2006; Koch et al., 2006; Ding et al., 2018). The double and triple mutants *npr1-1 FMO1-3D*, *npr4-4D FMO1-3D*, and *npr1-1 npr4-4D FMO1-3D* were isolated from the F2 progeny of a cross between *npr1-1 npr4-4D* and *FMO1-3D*, while *sid2-1 FMO1-3D* was isolated from the F2 progeny of a cross between *sid2-1* and *FMO1-3D*. Primers used for genotyping are listed in Supplemental Table 2. For SA-induced gene expression assays, plants were grown on half-strength Murashige and Skoog medium plates with 0.6% (w/v) agar at 23°C under cycles of 16 h of fluorescent light/8 h of dark (80 μE; Sylvania Octron 4100K, FO32/741/ECO bulbs). For pathogen-induced gene expression, measurement of metabolites, and pathogen growth assays, plants were grown on soil at 23°C under cycles of 12 h of fluorescent light/12 h of dark (100 μE; Philips Master TL5 HO 54W/840 bulbs).

Gene Expression Analysis

For RNA preparation, we collected ~50 mg of tissue from 4-week-old plants (four leaves from four different plants per replicate, for three independent biological replicates from different sets of plants) grown on soil or from 2-week-old seedlings (five to six whole seedlings per sample; three samples per genotype per treatment) grown on half-strength Murashige and Skoog medium plates. To analyze pathogen-induced gene expression, we collected the leaves of 4-week-old plants 24 h after infiltration with *Pseudomonas syringae* pv *maculicola* ES4326 (OD_{600} = 0.001), 12 h after infiltration with *Pseudomonas syringae* pv *tomato* DC3000 *hrcC* (OD_{600} = 0.05) or 10 mM $MgCl_2$ (mock), or 16 h after infiltration with *Pto* DC3000 *AvrRpt2* (OD_{600} = 0.005), *Pto* DC3000 *AvrRps4* (OD_{600} = 0.005), or 10 mM $MgCl_2$. Total RNA was extracted from all samples using the EZ-10 Spin Column Plant RNA Mini-Preps Kit (BIO BASIC CANADA). RT was performed using the EasyScript Reverse Transcriptase (ABM), and qPCR was performed using the Takara SYBR Premix Ex (Clontech) following the manufacturers' instructions. We normalized relative expression values to *ACTIN1*. Primer sequences used for qPCR are listed in Supplemental Table 2.

Measurement of Pip and NHP

To induce the production of Pip and NHP, we collected the leaves of 4-week-old plants 24 h after infiltration with *Psm* ES4326 (OD_{600} = 0.001) or 10 mM $MgCl_2$ (mock). Each treatment consisted of three independent samples from each genotype, each constituting ~75 mg of treated leaf tissue from six individual plants; a total of 18 plants per genotype/treatment were sampled. We extracted Pip using the EZ:faast free amino acid analysis kit, with norvalene as internal standard (Phenomenex). Pip detection and quantification were performed on a gas chromatography-mass spectrometry system (Agilent, 5973N) as previously described, with minor modifications (Návarová et al., 2012). A ZB-AAA capillary column (Zebron, Phenomenex; 10 m × 0.25 mm i.d.) and the following oven program were used: on-column injection at 50°C, oven temperature maintained at 50°C for 2 min, raised by 30°C/min to 320°C, and held for 2 min at 320°C. A constant helium flow of 1.4 mL/min was maintained during the entire program.

We extracted NHP using a previously described procedure (Hartmann et al., 2018) with some modifications. Briefly, ~75 mg of leaf tissue was ground and extracted once with 0.6 mL of 90% (v/v) methanol, with 0.5 μg of 2-hydroxy-cyclohexanecarboxylic acid (2-HCC; Sigma-Aldrich) added to each sample as internal standard. After gently shaking at 4°C for 2 h, the samples were centrifuged at 12,000*g* for 5 min and the supernatants were transferred to new tubes. We extracted the remaining pellets again with 0.6 mL of methanol and centrifuged as above, and the new supernatant was combined with the first. We took out an aliquot of 300 μL per sample, evaporated the solvent under a stream of nitrogen, and subjected the resulting residue to chemical derivatization by adding 20 μL of pyridine and 20 μL of *N*,*O*-bis(trimethylsilyl)trifluoroacetamide (Sigma-Aldrich). The reaction mixtures were incubated at 70°C for 30 min, cooled and kept at room temperature for 30 min, and finally diluted with 60 μL of hexane and transferred into gas chromatography vials. We injected 0.2 μL of each sample for analysis on a gas chromatography-mass spectrometry system (Agilent, 5973N) equipped with an HP-1 capillary column (Agilent; 30 m × 0.32 mm i.d.) using the following oven program: on-column injection at 70°C, oven held for 2 min at 70°C, raised by 10°C/min to 320°C, and held for 5 min at 320°C.

NHP, 2-HCC, and NHP-*OG* were analyzed based on their characteristic fragment ions *m/z* 172, 273, and 652, respectively. To determine the amount of individual metabolites, we integrated their peak areas in selected ion chromatograms using MSD ChemStation software (Agilent) and compared them with the peak area of the corresponding internal standard (IS): Pip (*m/z* 170)/IS norvalene (*m/z* 158); NHP (*m/z* 172)/IS 2-HCC (*m/z* 273), using correction factors for each pair of compounds experimentally determined with authentic standards. The presence of NHP-*OG* was determined based on its mass spectral characteristics (*m/z* 172 and 652). Because an authentic standard for NHP-*OG* was not available, relative NHP-*OG* abundances were determined by quantifying peak areas of its molecular ion *m/z* 652 relative to those of 2-HCC fragment *m/z* 273 in respective selected ion chromatograms.

2,5-DHBA and SA Quantification

For 2,5-DHBA and SA measurements, we collected two leaves each from six 4-week-old plants 16 h after infiltration with *Pto* DC3000 *AvrRpt2* (OD_{600} = 0.005) or 10 mM $MgCl_2$ (mock). For each treatment, four independent samples were collected, each sample constituting ~100 mg of leaf tissue from six individual plants, for a total of 24 plants per genotype/treatment. 2,5-DHBA, free SA, and total SA were extracted using previously described

protocols (Zhang et al., 2017). Samples were analyzed using an HPLC device (1200 series, Agilent) equipped with a C18 column (5 μm, 4.6 × 150 mm; Eclipse XDB, Agilent) and a fluorescence detector (G1321A, Agilent). 2,5-DHBA, free SA, and total SA were quantified using ISs and as previously described with modifications (Zhang et al., 2017). The mobile phase contained 0.2 M KOAc, 0.5 mM EDTA, pH 5.0, and methanol. For SA analysis, we included 6% (v/v) methanol and selected 295 and 405 nm as excitation and emission wavelengths, respectively. For 2,5-DHBA measurement, methanol was maintained at 3% (v/v), with excitation and emission wavelengths of 320 and 449 nm, respectively. The flow rate was fixed at 1 mL/min, and 5 μL of sample was injected in both cases. We determined target compound concentrations by calculating the peak areas in plant samples relative to those of corresponding synthetic standards.

ChIP-qPCR Analysis

ChIP assays were performed following a previously described protocol (Sun et al., 2015). Specifically, we cross-linked 2-week-old seedlings from Col-0 and *tga2 tga5 tga6* and collected the tissue for ChIP. Anti-TGA2 antibodies specifically recognizing proteins of clade II members of the TGA family, TGA2, TGA5, and TGA6 (Ding et al., 2018), and protein A-agarose beads (GE Healthcare) or protein A-agarose beads alone (no-antibody control) were used to pull down the chromatin complexes containing TGA2/5/6 proteins. Two independent batches of samples were used, and each sample was divided into four aliquots, two for no-antibody controls and two with anti-TGA2 antibodies for the ChIP samples. We performed qPCR with the immunoprecipitated DNA as template using primers specific to promoters of selected genes. Sequences of primers for ChIP-qPCR are listed in Supplemental Table 2.

Bacterial Pathogen Infection Assays

For bacterial pathogen infection assays, two leaves each from two 4-week-old plants were infiltrated with bacterial suspension in 10 mM $MgCl_2$: *Pto* DC3000 *hrcC* (OD_{600} = 0.002), *Pto* DC3000 *AvrRpt2* (OD_{600} = 0.0005), and *Pto* DC3000 *AvrRps4* (OD_{600} = 0.0005). We collected infected leaves 1 h (on day 0) and 3 d after inoculation. Two leaf discs from two infected leaves of one plant were collected as one sample, and six samples were analyzed for each genotype for day 3, while three to four samples were used for day 0. Samples were ground, serially diluted, and plated on Luria-Bertani agar plates to determine colony-forming units. For flg22-triggered protection assays, two leaves each from 4-week-old plants were infiltrated with water or 1 μM flg22. After 24 h, we infiltrated the pretreated leaves with *Pto* DC3000 at a cell density of OD_{600} = 0.001 in 10 mM $MgCl_2$. After inoculation with *Pto* DC3000 for 3 d, we determined bacterial titers in infected leaves as above.

Oomycete Pathogen Infection Assays

We performed the SAR assay with the oomycete pathogen *Hyaloperonospora arabidopsidis* Noco2 as previously reported (Zhang et al., 2010). Briefly, two primary leaves from 3-week-old plants were infiltrated with *Psm* ES4326 (OD_{600} = 0.001) or 10 mM $MgCl_2$. After 2 d, we sprayed whole plants with *Hpa* Noco2 spore suspension at a titer of 50,000/mL in water, using 15 plants per genotype per treatment. Inoculated plants were covered with a clear plastic dome and incubated at 18°C in a 12-h/12-h light/dark cycle in a growth chamber for 1 week. Disease symptoms were scored by counting the number of conidiophores on the distal leaves; we assigned disease rating scores as described in the legend of Figure 1A.

For NHP-induced immunity against *Hpa* Noco2, we infiltrated two primary leaves from 3-week-old plants with 1 mM NHP or water (mock). After 24 h, plants were sprayed with *Hpa* Noco2 spore suspension (50,000/mL in water), using 15 plants for each treatment. Disease symptoms were scored 7 d after inoculation as described above.

For *Hpa* Noco2 infection on seedlings, 2-week-old soil-grown seedlings were sprayed with *Hpa* Noco2 spore suspension (50,000/mL in water). Inoculated plants were covered with a clean dome and grown at 18°C under a 12-h/12-h light/dark cycle in a growth chamber. *Hpa* Noco2 sporulation was counted 7 d later.

[^{3}H]SA Binding Assays

We purified recombinant His_6-MBP-NPR1 and His_6-MBP-NPR4 proteins for [^{3}H]SA binding assay by size-exclusion chromatography, as previously described (Ding et al., 2018). Size-exclusion columns were prepared by adding 0.13 g of Sephadex G-25 (GE Healthcare) to a Qiagen shredder column and preequilibrated with PBS buffer containing 0.1% (v/v) Tween 20 overnight at 4°C; excess buffer was removed by spinning at 735*g* for 2 min before use.

The binding reactions were performed by incubating 0.4 mg/mL (w/v) His_6-MBP-NPR1 or His_6-MBP-NPR4 protein with 200 nM [^{3}H]SA (American Radiolabeled Chemicals; specific activity 30 Ci/mmol) in 50 μL of PBS buffer on ice for 1 h. Unlabeled SA or NHP was added to the reaction mixture at 2 mM (10,000-fold excess over [^{3}H]SA). After incubation, the reaction mixtures were loaded onto the columns and centrifuged immediately as above. The radioactivity in the flow-through fraction (bound [^{3}H]SA) was measured using a scintillation counter (LS6500, Beckman Coulter).

Accession Numbers

Sequence data for most genes studied in this article can be found in the Arabidopsis Genome Initiative database under the following accession numbers: *ACTIN1* (At2g37620), *ALD1* (At2g13810), *CBP60g* (At5g26920), *DMR6* (At5g24530), *EDS5* (At4g39030), *FMO1* (At1g19250), *NPR1* (At1g64280), *NPR4* (At4g19660), *PBS3* (At5g13320), *PR1* (At2g14610), *PR2* (At3g57260), *SARD1* (At1g73105), *SID2/ICS1* (At1g74710), *UGT76B1* (At3g11340), *UGT74F1* (At2g43840), and *UGT74F2* (At2g43820).

Supplemental Data

Supplemental Figure 1. Induction of *UGT74F1* in wild-type, *npr1-1*, *npr4-4D* and *npr1-1 npr4-4D* plants by *Pto* DC3000 *AvrRpt2*. (Supports Figure 6).

Supplemental Figure 2. Induction of *ICS1*, *EDS5* and *PBS3* expression by SA and ChIP-PCR analysis of binding of TGA2 to their promoter regions. (Supports Figure 6)

Supplemental Figure 3. Induction of *CBP60g* in Col-0 (wild type), *npr1-1*, *npr4-4D* and *npr1-1 npr4-4D* plants by *Pto* DC3000 *AvrRpt2*. (Supports Figure 6).

Supplemental Table 1. TGACG motifs in promoter regions of genes involved in NHP/SA biosynthesis and metabolism.

Supplemental Table 2. Primers used in this study.

ACKNOWLEDGMENTS

We thank Jane Parker (Max Planck Institute for Plant Breeding Research) for *fmo1-1 sid2-1* and *eds1-2* (Col-0) seeds. This work was supported by the Natural Sciences and Engineering Research Council (NSERC) Discovery Grant Program (grants to Y.Z., X.L., and R.J.), the NSERC CREATE Grant Program (grant PRoTeCT to Y.Z. and X.L.), the National Natural Science Foundation of China (grant 31670277 to K.Z.), University of British Columbia (4YF PhD scholarship to Y.L.), and Hunan Agricultural University (to Y.L.).

AUTHOR CONTRIBUTIONS

Y.L., T.S., K.Z., R.J., and Y.Z. planned and designed the research; Y.L., T.S., Y.S., Y.J.Z., H.T., J.L., S.C., X.H., A.R., Y.D., and A.R.O. performed experiments and analyzed data; T.S., Y.L., Y.S., K.Z., X.L., R.J., and Y.Z. wrote the article.

Received June 30, 2020; revised September 21, 2020; accepted October 5, 2020; published October 9, 2020.

REFERENCES

Aarts, N., Metz, M., Holub, E., Staskawicz, B.J., Daniels, M.J., and Parker, J.E. (1998). Different requirements for EDS1 and NDR1 by disease resistance genes define at least two R gene-mediated signaling pathways in Arabidopsis. Proc. Natl. Acad. Sci. USA **95:** 10306–10311.

Bartsch, M., Gobbato, E., Bednarek, P., Debey, S., Schultze, J.L., Bautor, J., and Parker, J.E. (2006). Salicylic acid-independent ENHANCED DISEASE SUSCEPTIBILITY1 signaling in Arabidopsis immunity and cell death is regulated by the monooxygenase FMO1 and the Nudix hydrolase NUDT7. Plant Cell **18:** 1038–1051.

Bauer, S., Mekonnen, D.W., Hartmann, M., Janowski, R., Lange, B., Geist, B., Zeier, J., and Schäffner, A.R. (2020). UGT76B1, a promiscuous hub of small molecule-based immune signaling, glucosylates N-hydroxypipecolic acid and controls basal pathogen defense. bioRxiv. Available at: https://doi.org/10.1101/2020.07.12.199356.

Cao, H., Bowling, S.A., Gordon, A.S., and Dong, X. (1994). Characterization of an Arabidopsis mutant that is nonresponsive to inducers of systemic acquired resistance. Plant Cell **6:** 1583–1592.

Century, K.S., Holub, E.B., and Staskawicz, B.J. (1995). NDR1, a locus of *Arabidopsis thaliana* that is required for disease resistance to both a bacterial and a fungal pathogen. Proc. Natl. Acad. Sci. USA **92:** 6597–6601.

Chen, Y.C., Holmes, E.C., Rajniak, J., Kim, J.G., Tang, S., Fischer, C.R., Mudgett, M.B., and Sattely, E.S. (2018). *N*-Hydroxy-pipecolic acid is a mobile metabolite that induces systemic disease resistance in *Arabidopsis*. Proc. Natl. Acad. Sci. USA **115:** E4920–E4929.

Cui, H., Tsuda, K., and Parker, J.E. (2015). Effector-triggered immunity: From pathogen perception to robust defense. Annu. Rev. Plant Biol. **66:** 487–511.

Delaney, T.P., Friedrich, L., and Ryals, J.A. (1995). Arabidopsis signal transduction mutant defective in chemically and biologically induced disease resistance. Proc. Natl. Acad. Sci. USA **92:** 6602–6606.

Delaney, T.P., Uknes, S., Vernooij, B., Friedrich, L., Weymann, K., Negrotto, D., Gaffney, T., Gut-Rella, M., Kessmann, H., Ward, E., and Ryals, J. (1994). A central role of salicylic acid in plant disease resistance. Science **266:** 1247–1250.

Després, C., DeLong, C., Glaze, S., Liu, E., and Fobert, P.R. (2000). The Arabidopsis NPR1/NIM1 protein enhances the DNA binding activity of a subgroup of the TGA family of bZIP transcription factors. Plant Cell **12:** 279–290.

Ding, P., Rekhter, D., Ding, Y., Feussner, K., Busta, L., Haroth, S., Xu, S., Li, X., Jetter, R., Feussner, I., and Zhang, Y. (2016). Characterization of a pipecolic acid biosynthesis pathway required for systemic acquired resistance. Plant Cell **28:** 2603–2615.

Ding, Y., Sun, T., Ao, K., Peng, Y., Zhang, Y., Li, X., and Zhang, Y. (2018). Opposite roles of salicylic acid receptors NPR1 and NPR3/NPR4 in transcriptional regulation of plant immunity. Cell **173:** 1454–1467.e1415.

Fan, W., and Dong, X. (2002). In vivo interaction between NPR1 and transcription factor TGA2 leads to salicylic acid-mediated gene activation in Arabidopsis. Plant Cell **14:** 1377–1389.

Fu, Z.Q., and Dong, X. (2013). Systemic acquired resistance: Turning local infection into global defense. Annu. Rev. Plant Biol. **64:** 839–863.

Fu, Z.Q., Yan, S., Saleh, A., Wang, W., Ruble, J., Oka, N., Mohan, R., Spoel, S.H., Tada, Y., Zheng, N., and Dong, X. (2012). NPR3 and NPR4 are receptors for the immune signal salicylic acid in plants. Nature **486:** 228–232.

Gaffney, T., Friedrich, L., Vernooij, B., Negrotto, D., Nye, G., Uknes, S., Ward, E., Kessmann, H., and Ryals, J. (1993). Requirement of salicylic acid for the induction of systemic acquired resistance. Science **261:** 754–756.

Gómez-Gómez, L., and Boller, T. (2000). FLS2: An LRR receptor-like kinase involved in the perception of the bacterial elicitor flagellin in Arabidopsis. Mol. Cell **5:** 1003–1011.

Hartmann, M., Kim, D., Bernsdorff, F., Ajami-Rashidi, Z., Scholten, N., Schreiber, S., Zeier, T., Schuck, S., Reichel-Deland, V., and Zeier, J. (2017). Biochemical principles and functional aspects of pipecolic acid biosynthesis in plant immunity. Plant Physiol. **174:** 124–153.

Hartmann, M., Zeier, T., Bernsdorff, F., Reichel-Deland, V., Kim, D., Hohmann, M., Scholten, N., Schuck, S., Brautigam, A., Holzel, T., Ganter, C., and Zeier, J. (2018). Flavin monooxygenase-generated N-hydroxypipecolic acid is a critical element of plant systemic immunity. Cell **173:** 456–469.e416.

Huang, W., Wang, Y., Li, X., and Zhang, Y. (2020). Biosynthesis and regulation of salicylic acid and N-hydroxypipecolic acid in plant immunity. Mol. Plant **13:** 31–41.

Jones, J.D., and Dangl, J.L. (2006). The plant immune system. Nature **444:** 323–329.

Koch, M., Vorwerk, S., Masur, C., Sharifi-Sirchi, G., Olivieri, N., and Schlaich, N.L. (2006). A role for a flavin-containing monooxygenase in resistance against microbial pathogens in Arabidopsis. Plant J. **47:** 629–639.

Li, X., Kapos, P., and Zhang, Y. (2015). NLRs in plants. Curr. Opin. Immunol. **32:** 114–121.

Mohnike, L., Rekhter, D., Huang, W., Feussner, K., Tian, H., Herrfurth, C., Zhang, Y., and Feussner, I. (2020). The glycosyltransferase UGT76B1 is critical for plant immunity as it governs the homeostasis of N-hydroxy-pipecolic acid. bioRxiv. Available at: https://doi.org/10.1101/2020.06.30.179960.

Návarová, H., Bernsdorff, F., Döring, A.-C., and Zeier, J. (2012). Pipecolic acid, an endogenous mediator of defense amplification and priming, is a critical regulator of inducible plant immunity. Plant Cell **24:** 5123–5141.

Noutoshi, Y., Okazaki, M., Kida, T., Nishina, Y., Morishita, Y., Ogawa, T., Suzuki, H., Shibata, D., Jikumaru, Y., Hanada, A., Kamiya, Y., and Shirasu, K. (2012). Novel plant immune-priming compounds identified via high-throughput chemical screening target salicylic acid glucosyltransferases in Arabidopsis. Plant Cell **24:** 3795–3804.

Radojičić, A., Li, X., and Zhang, Y. (2018). Salicylic acid: A double-edged sword for programed cell death in plants. Front. Plant Sci. **9:** 1133.

Rekhter, D., Lüdke, D., Ding, Y., Feussner, K., Zienkiewicz, K., Lipka, V., Wiermer, M., Zhang, Y., and Feussner, I. (2019). Isochorismate-derived biosynthesis of the plant stress hormone salicylic acid. Science **365:** 498–502.

Rochon, A., Boyle, P., Wignes, T., Fobert, P.R., and Després, C. (2006). The coactivator function of Arabidopsis NPR1 requires the core of its BTB/POZ domain and the oxidation of C-terminal cysteines. Plant Cell **18:** 3670–3685.

Sattely, E., Holmes, E., Chen, Y.C., and Mudgett, M.B. (2020). Arabidopsis UGT76B1 glycosylates N-hydroxy-pipecolic acid and inactivates systemic acquired resistance in tomato. bioRxiv https://doi.org/10.1101/2020.07.06.189894.

Sun, T., Busta, L., Zhang, Q., Ding, P., Jetter, R., and Zhang, Y. (2018). TGACG-BINDING FACTOR 1 (TGA1) and TGA4 regulate salicylic acid and pipecolic acid biosynthesis by modulating the expression of SYSTEMIC ACQUIRED RESISTANCE DEFICIENT 1 (SARD1) and CALMODULIN-BINDING PROTEIN 60g (CBP60g). New Phytol. **217:** 344–354.

Sun, T., et al. (2020). Redundant CAMTA transcription factors negatively regulate the biosynthesis of salicylic acid and N-hydroxypipecolic acid by modulating the expression of SARD1 and CBP60g. Mol. Plant **13:** 144–156.

Sun, T., Zhang, Y., Li, Y., Zhang, Q., Ding, Y., and Zhang, Y. (2015). ChIP-seq reveals broad roles of SARD1 and CBP60g in regulating plant immunity. Nat. Commun. **6:** 10159.

van Damme, M., Huibers, R.P., Elberse, J., and Van den Ackerveken, G. (2008). Arabidopsis DMR6 encodes a putative 2OG-Fe(II) oxygenase that is defense-associated but required for susceptibility to downy mildew. Plant J. **54:** 785–793.

Vlot, A.C., Dempsey, D.A., and Klessig, D.F. (2009). Salicylic acid, a multifaceted hormone to combat disease. Annu. Rev. Phytopathol. **47:** 177–206.

Wang, L., Tsuda, K., Sato, M., Cohen, J.D., Katagiri, F., and Glazebrook, J. (2009). Arabidopsis CaM binding protein CBP60g contributes to MAMP-induced SA accumulation and is involved in disease resistance against *Pseudomonas syringae*. PLoS Pathog. **5:** e1000301.

Wang, L., Tsuda, K., Truman, W., Sato, M., Nguyen, V., Katagiri, F., and Glazebrook, J. (2011). CBP60g and SARD1 play partially redundant critical roles in salicylic acid signaling. Plant J. **67:** 1029–1041.

Wang, Y., Schuck, S., Wu, J., Yang, P., Döring, A.C., Zeier, J., and Tsuda, K. (2018). A MPK3/6-WRKY33-ALD1-pipecolic acid regulatory loop contributes to systemic acquired resistance. Plant Cell **30:** 2480–2494.

Wildermuth, M.C., Dewdney, J., Wu, G., and Ausubel, F.M. (2001). Isochorismate synthase is required to synthesize salicylic acid for plant defence. Nature **414:** 562–565.

Wu, Y., Zhang, D., Chu, J.Y., Boyle, P., Wang, Y., Brindle, I.D., De Luca, V., and Després, C. (2012). The Arabidopsis NPR1 protein is a receptor for the plant defense hormone salicylic acid. Cell Rep. **1:** 639–647.

Zhang, K., Halitschke, R., Yin, C., Liu, C.J., and Gan, S.S. (2013). Salicylic acid 3-hydroxylase regulates Arabidopsis leaf longevity by mediating salicylic acid catabolism. Proc. Natl. Acad. Sci. USA **110:** 14807–14812.

Zhang, Y., Cheng, Y.T., Qu, N., Zhao, Q., Bi, D., and Li, X. (2006). Negative regulation of defense responses in Arabidopsis by two NPR1 paralogs. Plant J. **48:** 647–656.

Zhang, Y., Fan, W., Kinkema, M., Li, X., and Dong, X. (1999). Interaction of NPR1 with basic leucine zipper protein transcription factors that bind sequences required for salicylic acid induction of the PR-1 gene. Proc. Natl. Acad. Sci. USA **96:** 6523–6528.

Zhang, Y., and Li, X. (2019). Salicylic acid: Biosynthesis, perception, and contributions to plant immunity. Curr. Opin. Plant Biol. **50:** 29–36.

Zhang, Y., Tessaro, M.J., Lassner, M., and Li, X. (2003). Knockout analysis of Arabidopsis transcription factors TGA2, TGA5, and TGA6 reveals their redundant and essential roles in systemic acquired resistance. Plant Cell **15:** 2647–2653.

Zhang, Y., Xu, S., Ding, P., Wang, D., Cheng, Y.T., He, J., Gao, M., Xu, F., Li, Y., Zhu, Z., Li, X., and Zhang, Y. (2010). Control of salicylic acid synthesis and systemic acquired resistance by two members of a plant-specific family of transcription factors. Proc. Natl. Acad. Sci. USA **107:** 18220–18225.

Zhang, Y., Zhao, L., Zhao, J., Li, Y., Wang, J., Guo, R., Gan, S., Liu, C.J., and Zhang, K. (2017). *S5H/DMR6* encodes a salicylic acid 5-hydroxylase that fine-tunes salicylic acid homeostasis. Plant Physiol. **175:** 1082–1093.

Zhou, J.M., Trifa, Y., Silva, H., Pontier, D., Lam, E., Shah, J., and Klessig, D.F. (2000). NPR1 differentially interacts with members of the TGA/OBF family of transcription factors that bind an element of the PR-1 gene required for induction by salicylic acid. Mol. Plant Microbe Interact. **13:** 191–202.

Zhou, J.M., and Zhang, Y. (2020). Plant immunity: Danger perception and signaling. Cell **181:** 978–989.

Zipfel, C. (2014). Plant pattern-recognition receptors. Trends Immunol. **35:** 345–351.